Ultrafast Rearrangement of Norbornene Excited at 200 nm

W. Fuss,*,† K. K. Pushpa,† W. E. Schmid,† and S. A. Trushin†,‡

Max-Planck-Institut für Quantenoptik, D-85741 Garching, Germany and B.I. Stepanov Institute of Physics, Belarus Academy of Sciences, 220602 Minsk, Belarus

Received: May 14, 2001; In Final Form: August 9, 2001

By exciting norbornene (bicyclo[2,2,1]heptene) in the gas phase at 200 nm and probing it by nonresonant multiphoton ionization with mass-selective detection of the ion yields, we found five time constants τ_i (30, 60, 52, 800 fs, and 92 ps). $\tau_1-\tau_3$ represent traveling times through observation windows on excited surfaces, whereas τ_4 and τ_5 reflect processes in the hot ground state. We assign τ_1 to departure from the Franck−Condon region of the $\pi\pi^*$ state populated at 200 nm, and τ_2 to traveling along the $\pi\pi^*$ surface. To explain the subsequent window (τ_3), we suggest that the $\pi\pi^*$ surface is crossed by the zwitterionic state Z and that the two known carbene products form from this state. The carbenes then stabilize on the ground-state surface within τ_4 and τ_5 to form the two known photoproducts. − The fragmentation pattern showed that cyclopentadiene was not detected until at least 600 ps. Hence the retro-Diels−Alder reaction, known to be allowed in the ground state, probably takes longer.

1. Introduction

The photochemistry of many monoalkenes is surprisingly rich (reviews[1−4]). Unimolecular purely photochemical reactions comprise cis−trans isomerization, pericyclic reactions, formation of carbenes (which form consecutive products in ground-state reactions) and sometimes dissociation (e.g., elimination of an H atom). In addition, in the gas phase, one observes reactions in the hot ground state of the reactant (formed by internal conversion accompanying the above reactions) or of products; such reactions can be suppressed by collisions, in particular in solution; this criterion can be used to distinguish such reactions from the purely photochemical ones (see, for example,[2]) As compared with this variability, norbornene is a very simple case: The only known unimolecular reactions that can be classified photochemical involve formation of two carbenes, one of which stabilizes by insertion into a CH bond giving a tricyclic compound, the other giving a ring-contraction product (see reaction scheme).[1,5,6] Norbornene hence appears appropriate to investigate the dynamics of carbene formation.

It is interesting that electron-accepting substituents at the double bond of norbornene suppress carbene formation in favor of a pericyclic reaction (1,3-sigmatropic shift of the CH_2 bridge).[1,3,4] This observation was believed to indicate that carbenes form preferentially from a Rydberg state, which is lower than the $\pi\pi^*$ state in norbornene, but is raised by the electronegative substituents.[7] We suggest here a much later decision (via a zwitterionic state), which is more consistent with the results on ultrafast dynamics. This is also predicted by very recent CASSCF calculations which localized conical intersections (CoIns) between the zwitterionic and ground states for carbene formation from norbornene, cyclohexene and ethylene.[8]

Although not observed yet in unsubstituted norbornene, 1,3-sigmatropic shifts seem to be a possibility also in this system at slightly higher energies. This is suggested by quantum-chemical calculations of the pertinent CoIns and other features

SCHEME 1: Quantum Yields $\phi_1 = \phi_2 = 7\%$[5] or 2% (adjusted in ref 1)

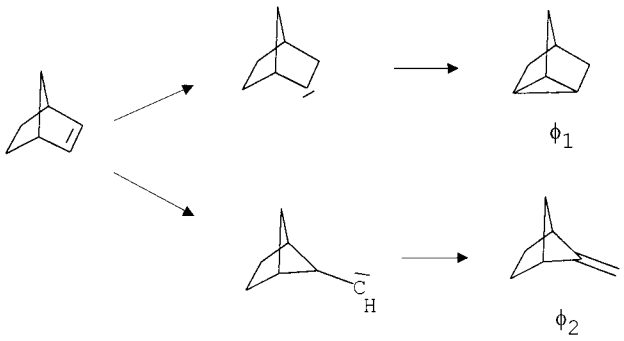

of the potential energy surfaces.[9] The geometry and electronic structure at one of these intersections was also suggested to enable an ultrafast stepwise retro-Diels−Alder reaction (products: cyclopentadiene + ethylene); the calculation was hence believed to support such an assignment of previous ultrafast spectroscopy of norbornene and cyclohexene.[10,11] However, we could not detect cyclopentadiene until 600 ps and conclude that, as in cyclohexene,[12] the retro-Diels−Alder reaction probably takes longer time. The end products of this reaction were actually observed;[13] they can be formed in the ground state with an activation energy of 1.98 eV and preexponential factor of 4×10^{14} s^{-1}.[14]

The UV spectrum of norbornene[15] is typical of alkyl substituted olefins:[16,17] The first strong absorption corresponds to a $\pi \rightarrow \pi^*$ excitation; it has a maximum at 196 nm, containing some vibrational structure, and an exponential wing extending to beyond 220 nm (as measured with saturated vapor in a 10-cm cell). A weak precursor band with more pronounced vibrational structure (0−0 band at 207.7 nm) on top of this wing is assigned to a Rydberg $\pi \rightarrow$ 3s transition which contains some admixed $\pi\sigma^*$ character.[7,16] Excitation at 200 nm practically only populates the $\pi\pi^*$ state. The vertical ionization energy is 8.95 eV according to vacuum UV studies,[17] whereas the photoelectron spectrum indicates a slightly higher value (9.2 eV).[7]

† Max-Planck-Institut für Quantenoptik.
‡ B.I. Stepanov Institute of Physics, Belarus Academy of Sciences.

10.1021/jp011843v CCC: $20.00
Published on Web 11/03/2001

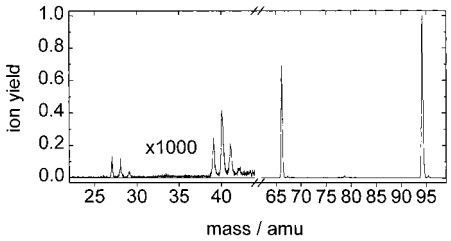

Figure 1. Transient mass spectrum of norbornene recorded by photoionization by 800 nm at 80 fs after pumping by 200 nm. At this delay time, fragmentation reaches its maximum. The ion yields are normalized to the parent ion (94 amu).

2. Experimental Method and Evaluation

The molecules were pumped in the gas phase (pressure varied from 10^{-9} to 10^{-4} mbar) at room temperature by a frequency-quadrupled pulse of a Ti-sapphire laser system (200 nm, 150 fs fwhm, 10^9 W cm^{-2}) and then probed by nonresonant multiphoton dissociative ionization at the fundamental wavelength (800 nm, 110 fs, 10^{13} W cm^{-2}). The two beams were linearly polarized with an angle of 55° ("magic angle") between each other in order to avoid time dependences induced by molecular rotation. In each pulse, two ion signals were simultaneously measured by two boxcar integrators: besides an ion from norbornene (sec. 3) also Xe^+ which is due to nonresonant (1+4)-multiphoton ionization of Xe; it gives the time zero—the maximum of the Gaussian fit function—with precision ± 1 fs and serves for synchronization of different scans with accuracy ± 2 fs. This error was found for the reproducibility from run to run in typically 10 runs.

For evaluation, we assume that the molecule sequentially reaches several locations i (observation windows) on the potential energy surfaces with lifetime τ_i. Since these times turn out to be very short (<100 fs), the transit time through the window gives a significant contribution to τ_i. Therefore, we do not distinguish "lifetime" (time constant) from "traveling (transit) time". The signals are then expressed as a sum of exponentials (with time constants τ_i) convoluted with the (Gaussian) pump and probe pulses. The exponential part of each signal is proportional to a linear combination of the time-dependent populations (which themselves are sums of exponentials) of each window, the coefficient being the cross-section ${}^m\sigma_i$ to produce an ion of mass m from window i.

The experimental setup, special features of transient dissociative ionization including the effective time resolution and the method of assignment are discussed in ref 18, in less detail also in refs 19−21 and briefly reviewed in ref 22.

Norbornene was used as commercially available (Fluka, stated purity 97%). Taking a sample from the gas phase, we did not detect any impurity above 0.1% by gas-chromatography.

3. Results

Figure 1 shows the fragmentation pattern observed 80 fs after the pump pulse with the relative strength of the signals. Around this delay time, fragmentation is maximum. The transient signals for Xe^+ (which gives the time zero and an indication of the instrumental function), the parent ion (mass 94) and typical fragment ions (mass 66 and 40) for norbornene are given in Figure 2 in a linear and a logarithmic scale. Several neutral precursors (locations on the potential energy surfaces) must be assumed because the signals are obviously not proportional to each other. This is demonstrated, for instance by noncoincidence of the signal maxima, which are at 36, 69, and 111 fs for the masses 94, 66, and 40, respectively. The signals $C_7H_{10}^+$ and $C_5H_6^+$ (masses 94 and 66) only show a short spike decaying to

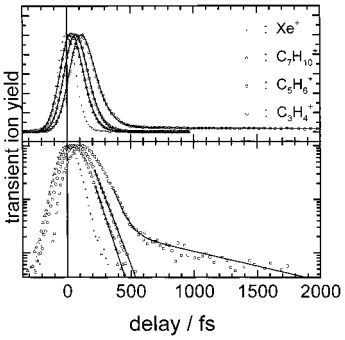

Figure 2. Typical time-resolved signals for norbornene on linear (top) and logarithmic (bottom) scales. The Xe^+ signal gives the time zero and approximately the instrumental function. Three time constants (τ_2, τ_4) can immediately be extracted from exponential tails (solid lines in the lower panel); similarly, the longer τ_5 is derived from the late-time signals (not shown) of the same light ions. Two more (τ_1, τ_3) are required to simulate (solid lines in the upper panel) the different delays of the rising wings. (The simulation used three consecutive processes, excluding the two slow ones, and convolution with the Gaussian instrumental function, see text). The signal at mass 41 (not shown) coincides with that of mass 40.

0. They are composed of the same two exponentials (time constants τ_1 and τ_2), but with weights differing in the two signals. Similarly, the signals with masses 41, 40, 39, 29, and 28 are composed of the same three exponentials (time constants $\tau_3-\tau_5$), but their weights differ in the various signals; in this case the first parts including the peaks even coincide. These light ions also show a weak (less than 1% of the maximum, see Figure 2) long-lived (> 600 ps) pedestal which is obviously due to an end product ("window 6").

The signals can be simulated by a sum of exponential time functions, convoluted with the (Gaussian) instrumental function (solid lines in Figure 2 top). Altogether, we receive 5 time constants $\tau_1-\tau_5$ (Table 1) by which all signals can be well reproduced. To derive them, we first determined from the singly exponential tail of the parent and mass-66 signals (Figure 2 bottom) a value of 60 fs (τ_2). Double exponential fits to the tails of the lighter fragments (mass ≤ 41) gave 60 fs (which is again τ_2, see below) and 800 fs (τ_4). The time constant τ_5 is derived from the long tail of the lighter fragments (in a separate investigation of the long delays) with singly exponential fits. It turned out that an additional time constant (τ_1) was necessary to reproduce the early appearance and the shape of the parent ion signal: Keeping τ_2 fixed, a doubly exponential fit (with convolution) of this signal gives τ_1. The corresponding simulation of the signals of mass 41, 40, and 28 gives the constraint $\tau_1 + \tau_3 = 82$ fs. Hence, $\tau_3 = 52$ fs, which is shorter than τ_2. In such a case, the observed decay of observation window 3 reflects the rate-determining decay of the preceding window, whereas the actual τ_3 can only be extracted from the rising part of the window-3 signals.

Sums of exponentials with up to 5 terms are the solutions of rate equations for populations in 6 observation windows or locations on the potential energy surfaces (the last one with infinite lifetime) connected by 5 consecutive processes. However, such a sum also results from kinetic description of a system with branching, i.e., of a set of consecutive and parallel reactions. Only the interpretation of the coefficients is then different. That is, purely mathematically, the 2 cases cannot be distinguished. The next section shows a satisfactory assignment using consecutive processes for $\tau_1-\tau_3$, followed by a branching with two parallel processes with time constants τ_4 and τ_5. For the purely sequential part, the fit procedure also provides the sequence (τ_2 after τ_1 etc.) of the processes.

TABLE 1: Lifetimes τ_i of the Locations *i* on the Potential Energy Surface and Cross-sections ${}^m\sigma_i$ for Generating Some Selected Ions (mass *m*) for Norbornene[a]

i	1	2	3	4	5	6
τ_i/fs	30 ± 10	60 ± 2	52 ± 10	800 ± 300	$(92 \pm 30) \times 10^3$	$>500 \times 10^3$
94 ($C_7H_{10}^+$)	1	0.19	0	0	0	0
66 ($C_5H_6^+$)	0.16	1	0	0	0	0
40 ($C_3H_4^+$)	0	0.074	1	0.012	0.007	0.002

[a] Nonzero values of ${}^m\sigma_i$ show from which signals (*m*) we deduced the time constants of the locations *i*. The error limits of τ_2, τ_4, and τ_5 are the standard deviations of the values determined in 10 runs from the singly (doubly) exponential fits to the tails of signals. The full fit also gives the constraint of $\tau_1 + \tau_3 = 80 \pm 5$ fs and $\tau_3 \leq \tau_2$, which implies the error limits of τ_1 and τ_3.

All time constants were independent of the *probe intensity* which was varied by a factor of 3, although the signal shapes were slightly affected, a change that can be described by intensity-dependent cross-sections for multiphoton ionization. The effective order for generating the parent ion by the probe was 1. Because two probe photons are required for ionization from the excited state (pumped by a photon of 6.2 eV, probe photon 1.55 eV, ionization energy 8.95−9.2 eV[7,17]), we can infer that the probe meets a resonance with a state near 7.75 eV which is partially saturated. In principle, the high intensity of the probe laser could lead to level shifts and thus perturb the pump process, perhaps even causing some artificial time dependence during the pump−probe overlapping time. However, the intensity independence shows that there is no reason to worry. We checked this point further in a separate experiment, monitoring the parent ion by probing by 400-nm pulses (110 fs) at much lower intensity ($\leq 10^{12}$ W cm^{-2}); this means, by one-photon probing. We found perfectly identical signals that are, of course, again well-fitted by the same two time constants τ_1 and τ_2 with the same ratio of ionization cross-sections. (Window 3 cannot be ionized by a single photon of 400 nm or 3.1 eV.)

The shape of the signals including the ratio of peak to pedestal did not depend on the *pump intensity* (varied by a factor of about 3). This is especially important for the pedestal (nonvanishing long-time signal) and proves that it is produced by a single pump photon.

The signal with mass 66 ($C_5H_6^+$) has been associated in the literature with production of neutral cyclopentadiene in a retro-Diels−Alder reaction.[10,11] The excess energy $E_{exc} = 6.2$ eV − reaction energy ≈ 5.4 eV would then be found distributed over the products ethylene + cyclopentadiene. Therefore, we recorded the signals from cyclopentadiene without ($E_{exc} = 0$) and with pumping at 200 nm, probing at long delay when the excitation energy ($E_{exc} = 6.2$ eV) has been released. In both cases, the ratios of signals for mass 28 and 41 to mass 40 were ≤ 0.05. This is in contrast to norbornene, where all these ratios are 0.3−0.5 at any delay. This means that for norbornene the signals (including those for the end product) are at least not dominated by cyclopentadiene. That is, fragmentation of norbornene seems not detectable until about 600 ps. Additional evidence is deduced from the kinetics (sec. 4.1).

4. Discussion

Whereas for extracting time constants from the measured data it is not necessary to know the mechanism of ionization and fragmentation, such knowledge is helpful for assignment. In this way, it is even possible to conclude from experiment alone on properties of the potential energy surfaces. As previously shown for cyclohexadiene[18] or cycloheptatriene,[21] fragmentation only occurs in the ion. As the preceding paragraph shows, this is also justified in the present case. This fragmentation is caused by vibrational excess energy in the ion. (Note that the ions have plenty of time for this reaction—the time > 100 ns before acceleration—, whereas the neutrals only dispose on the fs-ps delay times.) There are three sources of such energy:[18] (1) Electronic relaxation down the potential surfaces releases kinetic (vibrational) energy in the neutral molecule, and ionization transfers most of this energy to the ion; i.e., a hot neutral gives rise to a hot ion. Hence, the fragmentation pattern allows to roughly estimate the vibrational energy (and thus also the electronic energy because the sum is constant) in the observation window of the neutral molecule. (2) Vertical ionization from a strongly displaced location leads to a high-lying part of the ionic potential surface. This is additional excess energy that contributes to fragmentation. (3) The ions themselves can absorb additional probe photons, thus giving rise to a distribution of excess energies. This is the reason each observation window gives a fragmentation pattern instead of a single fragment.

Also the signal intensities help in assignment, since the ionization probability strongly depends on electronic energy. As a rule, signals from the (hot or cold) ground state are always smaller by orders of magnitude than those from electronically excited states. The former also depend on a higher power of the probe intensity than the latter.

4.1. Assignment. The difference in signal intensity by more than 2 orders of magnitude shows that the first three time constants must belong to observation windows on excited-state surfaces, whereas τ_4 and τ_5 characterize processes on the ground-state surface. This is also supported by the dependence on the probe power: The relative ionization cross-sections for windows 4−6 increase by a factor 4−6 when the probe intensity is raised by a factor of 3. Furthermore, only small fragment ions are produced from windows 4−6, indicating that the neutral molecule in these windows is very hot and has hence released most of its electronic energy. Fragmentation continuously increases also from window 1 to 3, indicating release of electronic energy and/or displacement of the observation windows on the surfaces. τ_1 and τ_2 were from the parent-ion signal (and others). This means that these two windows must still be on a high-lying surface, certainly the $\pi\pi^*$ surface that was originally excited.

4.1.1. First Observation Window: Leaving from the Franck−Condon Region. Then the first time constant $\tau_1 = 30$ fs certainly represents traveling through, and leaving of, the Franck−Condon region. Slightly shorter times (10 fs) were found in 1,3-cyclohexadiene[18] and cycloheptatriene,[21] where this assignment was supported by comparable numbers deduced from the fluorescence quantum yields. The longer time in norbornene is consistent with the more pronounced vibrational structure[15] and its width of about 200 cm^{-1}; a lifetime of 30 fs would correspond to a homogeneous broadening of 167 cm^{-1}. A correlation of τ_1 with the width of vibrational structure has recently been observed in cyclohexadiene derivatives.[23]

4.1.2. Second Observation Window: Traveling on the $\pi\pi^*$ and Rydberg Surfaces and Leaving from There. In window 2, not more energy can have been released than about the fragmentation energy of the norbornene radical cation (to form

$C_5H_6^+$), which is about 0.4 eV.[24] The long-wavelength wing of the $\pi\pi^*$ absorption (extending to beyond 219 nm or 5.7 eV, see Introduction) shows that this surface reaches lower than about 0.5 eV below the pump-photon energy (6.2 eV). Hence this window does not belong to a lower state, but still lies on the (upper part of the) $\pi\pi^*$ surface. That is, τ_2 (= 60 fs) is the time for traveling (after the Franck−Condon region) along this surface and leaving to a lower state. However, we suggest that during the same τ_2 *part* of the population flows to the practically isoenergetic Rydberg state (207.7 nm, 5.97 eV); if it returns from there in a shorter time (but not much shorter, for consistency with the width of the vibrational structure, see below), it will not show up in the kinetics, and the signal will reflect only the sum of populations flowing in the two paths. Nevertheless, such a side path must be expected because the two surfaces are energetically close, but differ in their shift (as to conclude from the different structures in the two UV bands) so that they must intersect in an easily accessible CoIns. After the τ_2-window, the molecule must have left both states toward a lower-energy surface because the next window shows no parent ion anymore.

4.1.3. Third Observation Window: Traveling along a Zwitterionic Surface and Leaving from There. In contrast to windows 1 and 2, fragmentation after ionization from observation window 3 is already drastic: The heaviest ions observed are $C_3H_4^+$ (Table 1) and $C_3H_5^+$. Hence, this window must have a much lower energy (probably > 1 eV lower than the Franck−Condon region) and may also be more displaced from equilibrium geometry. Therefore, we must postulate such a lower excited state which should, however, be dark in one-photon absorption. We suggest it is the zwitterionic state (Z or π^{*2}) which involves excitation of two π electrons. In simple acyclic olefins this state is slightly below the $\pi\pi^*$ state at a twist angle of 90°,[25] but as suggested for cyclohexene[12] may be much lower than the latter in cyclic olefins where ring strain prevents large twist angles and lowering of the $\pi\pi^*$ state. In our case, we need two such CoIns differing in geometric structure to explain formation of the two different carbenes. Thus, we assign τ_3 = 52 fs to traveling along the Z surface, with the path branching and reaching these two CoIns.

It is known that in ethylene the Z/S_0 CoIn involves a partial H migration and supports formation of carbenes.[8,25−30] The recent calculation by Wilsey and Houk[8] also investigated norbornene and indeed found two such separate conical Z/S_0 CoIns, one with hydrogen migration, the other with carbon shift; for each, they localized three interconnected minima of the intersection space.

Recently, Soep et al. observed for a number of olefins in addition to short time constants ($\tau_1 \leq 100$ fs) in some cases also longer ones (τ_2 = 1.9−4 ps).[31] They used one-photon ionization (267 nm, 4.65 eV), detecting the parent-ion yield. For rationalizing the longer times, they suggested that a bottleneck is involved for reaching a CoIn. If this is the Z/S_0 CoIn, this long time represents the departure from the Z state. Because the signals are still parent ions, this assignment infers that the Z state is still high-lying, similarly as the $\pi\pi^*$ state. It is interesting that the long times were only observed in the acyclic olefins investigated, not in the two cyclic ones; according to the suggestions above, in the acyclic olefins there is indeed no reason the Z surface should be much lower than the $\pi\pi^*$ surface.

4.1.4. Final Observation Windows: Formation of the Carbenes and Consecutive Products. Formation of the two carbenes is completed on the ground-state surface after passing the CoIns. These two locations on the S_0 surface will not exchange population, but behave as two different species which can give rise to two different rates of decay and of formation of the two end products. We thus suggest that τ_4 and τ_5 are the times for stabilization of the two carbenes in their hot ground state. Norbornylidene was produced from other precursors in solution and was shown to react within the unusually short time of $\ll$ 100 ps[32] to the tricycloheptane of Scheme 1 exclusively.[33] In the gas phase, this time will be further shortened by the vibrational excess energy. Therefore, we assign the shorter lifetime τ_4 (= 0.8 ps) to norbornylidene and the longer τ_5 (= 92 ps) to the other carbene, bicyclo[2,2,1]hept-5-yl-carbene. (The latter will decay by H migration and possibly also back to norbornene; H migration times and activation energies in dialkylcarbenes are given e.g., in ref 34) In solution, due to cooling, the lifetimes of both carbenes will be longer than measured by us.

As an alternative we also considered the retro-Diels−Alder reaction of hot norbornene which forms from the CoIns along with the carbenes. However, already in section 3, it was mentioned that the fragmentation pattern does not support this possibility. Also, the kinetics of the small fragments suggests that it is not very probable: We found that all the ions with low masses investigated (41, 40, 29, 28) show the same time constants. (Only mass 40 is shown in Figure 2.) Hence, all these signals probably reflect the time behavior of the same neutral precursors (the two carbenes and end products, as claimed above). Because some of these masses are nearly absent in cyclopentadiene (the signal ratios mass-41/mass-40 and mass-28/mass-40 are < 0.05 at room temperature and after pumping at 200 nm and internal conversion, whereas this ratio in norbornene was 0.3−0.5 between 1 and 600 ps), the other small fragments can also not belong to this retro-Diels−Alder product. (Heavier fragments were absent at these long times.) That is, the retro-Diels−Alder reaction was not detected until 0.6 ns. A different interpretation would assume that mass 40 contains a contribution from cyclopentadiene (i.e., from another precursor) accidentally rising with about the same time constant τ_5 as the carbene (first precursor) decays. While we cannot exclude this possibility, we consider it less probable, since any cyclopentadiene produced should have a high ionization probability due to its low ionization energy and should hence give a rising mass-40 signal, instead of a decaying one as observed. On the other hand, an estimation with the Arrhenius parameters mentioned in the Introduction predicts a reaction time just in the range 10−100 ps for norbornene at 2470 K, a temperature corresponding to 6.2 eV of excess energy; an RRKM calculation would probably give a similar value. Further work seems necessary to clarify the actual time scale. But certainly it does not proceed in <1 ps (see next paragraph). Because all molecules have returned to the ground-state much before, the retro-Diels−Alder cleavage must be a ground-state reaction.

In this context, a comment on the time behavior of $C_5H_6^+$ (mass 66) may be appropriate. This ion was suggested to reflect the formation and decay of cyclopentadiene (to an unassigned product) in ref 11 or of a precursor of it in ref 10. However, in our experiment this signal shows exactly the same time constants (τ_1 and τ_2) as the parent ion, although the two exponentials have different weights in the two signals; hence these constants obviously belong to the intact molecule, not to a fragment. The different weights can be readily understood by taking into account that the efficiency of ionic photodissociation (by absorption of additional probe photons after ionization) differs at the two geometries corresponding to windows 1 and 2. A

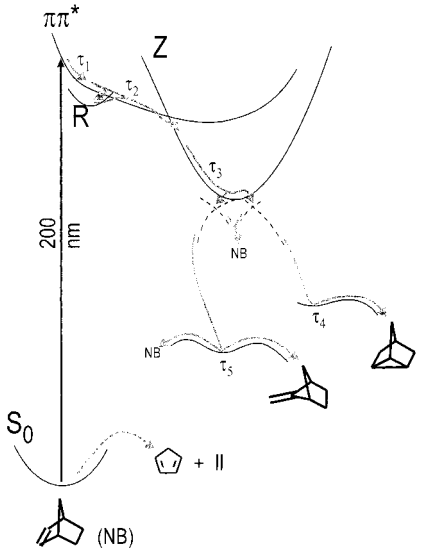

Figure 3. Suggested paths and potential energy surfaces. Initial excitation at 200 nm populates the Franck−Condon region of the $\pi\pi^*$ state. τ_i near the solid arrows represent the traveling times to which we assign the time constants extracted from the signals; τ_4 and τ_5 are the lifetimes of the carbenes (structures in Scheme 1). The broken arrow indicates the unobserved retro-Diels−Alder reaction. NB = norbornene. Coordinates are likely to involve C=C stretch during τ_1, pyramidalization of the sp^2 carbons during τ_2 and τ_3, and H or C migration in passing the S_1/S_0 conical intersections (crossing broken lines).

remarkable consequence of this mechanism is that the fragment signal shows up before the parent signal disappears, although the locations on the neutral's potential surface are consecutively populated. This possibility was not recognized in refs 10 and 11, where the early appearance of the fragment signal was believed to be evidence against consecutive processes, but in favor of two parallel retro-Diels−Alder reactions.

It may appear that some of the assignments might be examined by deuterium labeling. We refrained from such an attempt, however, because all the steps with hydrogen migration are accompanied by processes involving rearrangement of other moieties.

4.2. Potential Energy Surfaces, Coordinates and Geometries. The above assignments can be summarized in the schematic potential energy surfaces and pathways of Figure 3. The labels τ_i indicate the observation windows *i*. The short times $\tau_1-\tau_3$ are dominated by the traveling times through the windows indicated by the solid arrows, whereas τ_4 and τ_5 represent the times to overcome the barriers for stabilization of the carbenes. (For the structures of the latter, see the reaction scheme.)

Although the symmetry species of the $\pi\pi^*$ state is A″ in C_s, those of the other states is A′. Hence, the two indicated crossings of the excited states are symmetry-allowed, unless the distortion coordinate breaks C_s symmetry (see below). As every intersection, they must be conical. Some of the arrows hence indicate a path around the lower part of the double cone.

A detour via the Rydberg state, although not detected, must be postulated because there will be an easily accessible intersection between this and the $\pi\pi^*$ surface because the energies are similar while the displacements of the two surfaces strongly differ. In contrast to populating the Rydberg state from the higher $\pi\pi^*$ state, its lifetime is expected to be longer if it is populated by direct excitation of, for example, the 0−0 transition at 207.7 nm: The wave packet will meet a small barrier, as indicated in the figure. Indeed, picosecond lifetimes dependent on excess energy have been found when the Rydberg state of tetramethyl ethylene was excited.[35−37] We also interpret in this way the ultrafast data of ref 10 on norbornene excited at 209 nm which excites both the Rydberg 0−0 transition and the wing of the $\pi\pi^*$ band: The two signals observed (parent and mass-66 ions) probably each consist of contributions from the two states; only the longer lifetime (175−200 fs)[10], which we assign to the Rydberg state in the 0 vibrational level, can be directly extracted from the decaying part of both signals, whereas the shorter lifetime of the $\pi\pi^*$ state would only show up in simulation of the full signals including the rising part. Most data presented in ref 10, however, concern excitation at 8.1 eV. The states thus populated seem to have a similarly long lifetime, during which they probably relax to lower states such as $\pi\pi^*$. The shorter lifetime ($\tau_1 + \tau_2$ in the present work) of such a subsequent state cannot be deduced from such data.

The short τ_3 indicates that the conical S_1/S_0 CoIn(s) must also be easily accessible. We need two, to explain formation of the two different carbenes. They are indicated by broken lines in Figure 3, and the arrows for window 3 are curved, to emphasize the change of direction (leaving the drawing plane) of the pathway. The relative energies of the two carbenes (windows 4 and 5) are not known. Norbornylene stabilizes by forming a tricycloheptane (Scheme 1) practically exclusively.[33] For the other carbene, we also indicated the conceivable recovery of norbonene. The retro-Diels−Alder reaction from the hot S_0 of norbornene, unobserved by us, is indicated by a broken arrow.

The initial relaxation direction in the Franck−Condon region (observation window 1) certainly involves stretching of the CC double bond. In acyclic olefins this motion is accompanied or followed by CC twisting, since the lobes of the singly populated antibonding π^* orbital want to avoid each other. A twist is not possible in norbornene. However, as the calculation[9] shows, the lobes can also avoid each other by pyramidalization and rehybridization to sp^3, in particular if the distortion is antisymmetric, one H being displaced to the endo, the other to the exo direction. So after leaving the Franck−Condon region, the path will choose this direction. This tendency will even be more pronounced in the Z state (i.e., in window 3) which involves double excitation to π^*, and this state will therefore be more displaced. Because this coordinate is antisymmetric and breaks C_s symmetry, it will not lead to the real $\pi\pi^*$/Z crossing, but to an avoided crossing; i.e., it will lead around the lower cone, guiding the wave packet completely to the lower surface without branching. After sufficient excursion in this direction the two CH groups are nearly perpendicular to each other. This is a good prerequisite for H or C migration via intermediate structures with H or C bridge over the original double bond. In ethylene,[8,25−30] cyclohexene,[8,12] and norbornene, such bridged geometries are the structures at the Z/S_0 CoIns from where the carbenes are formed. It turned out that the twist angle between the two CH groups most favorable for the CoIn is clearly below 90°.[8,29,30] For norbornene, several interconnected minima of the CoIn space were found.[8] To explain our short τ_3, we suggest that only the CoIn structures requiring least motion will be easily accessed; that is those in which migration of H or C has just begun and in which the two CH groups are practically in cis orientation (see Figures 2 and 3 in ref 8).

In this context, it is worth noting that in ethylene it is the negatively charged C atom in the Z state which is the donor of the migrating H, whereas from the positively charged one migration meets a barrier.[26,27] If in norbornene a negative charge is stabilized at one carbon by a CF_3 or CN substituent, H migration from the other would hence require an activation energy. Furthermore, although the twisted (probably also the

pyramidalized) molecules in the zwitterionic state can be stabilized by polar substituents, the subsequent transition states cannot, because they are covalent.[26] This could explain why CF_3 or CN also suppress the carbene formed by C migration. The current interpretation[1,38] invokes the energetic lifting of the Rydberg state by these substituents; however, this explanation does not work in liquid phase where optical transition probabilities to Rydberg states are reduced by orders of magnitudes, although the substituent and wavelength effects have also been observed in solution.

5. Conclusion

The pathway suggested here for carbene formation is very similar to that for photochemical pericyclic reactions and cis−trans isomerizations (see, for example, ref 28): The molecule leaves the initially excited region along Franck−Condon active coordinates, then changes direction still on the spectroscopic surface, then passes over around a CoIn to a lower dark excited state, from where it leaves via CoIns to the ground-state surface of products and reactant. In the present experiment, the evidence for the dark state came from the fragmentation pattern in observation window 3, which showed the existence of an excited-state much lower in energy than the $\pi\pi^*$ and Rydberg states. We suggest it is the zwitterionic state Z. Already for cyclohexene we found evidence for such a state involved in formation of carbenes,[12] and the recent calculations of Wilsey and Houk strongly support this path.[8] Departure from this state is ultrafast (52 fs), and thereafter follow signals from the ground-state surface. That is, the pathway goes through conical intersections of the Z and S_0 surfaces. This is in contrast to the current belief that there is a direct pathway from the Rydberg state to the carbenes.[1,38] But a conical intersection of the S_0 and Rydberg surfaces is certainly not near the minimum of the latter since it is nearly not displaced from the S_0 minimum, as to judge from the nearly equal intensities of the 0−0 and 0−1 transitions in the Rydberg band. The present experiment clearly shows that the population flows via intermediate surfaces including that of the Z state.

We can infer that the decision between different products (and recovery of the reactant) is not (at least not exclusively) taken in the Franck−Condon region, but much later, probably mainly in the Z state. Substituent effects (section 4.2) and wavelength dependence (see ref 12) seem to be understandable on this basis. Because such effects are also observed in solution, invoking the Rydberg state for explanation was also not satisfactory because such states are suppressed (i.e., displaced to much higher energies and mixed with other states, so that the probability of optical excitation is much reduced) in the condensed phase (see e.g., ref 17). Although this was recognized in the previous debate as an argument against the model of early decision, the assumption of late decision could previously not explain wavelength and substituent dependences.

In this work, the dynamics were studied in the gas phase. The results can be transferred to solution if two effects are taken into account:

(1) Shift or distortion of electronic surfaces by the solvent. An example is the suppression of the Rydberg states (see above and sec. 4.2). Another one is the change of an activation energy by polarity effects mentioned in section 4.2.

(2) Cooling by the solvent, which typically takes a time of the order of 10 ps (see e.g., ref 39 and references quoted). Therefore, the excited-state processes that all take $\ll$1 ps are not affected. But the carbene rearrangements will be slowed (section 4.2) and hot-ground-state reactions can be completely suppressed in solution. The retro-Diels−Alder cleavage is suggested to be to such a thermal reaction. It is also worth noting that in the absence of effects of type 1, the subpicosecond dynamics will be generally the same in the gas phase and in solution.

Acknowledgment. We thank K.N. Houk for stimulating discussions and for making available results before publication[8] and a referee for drawing our attention to refs 32,33.

References and Notes

(1) Kropp, P. J. Photorearrangement and fragmentation of alkenes. In *Handbook of Organic Photochemisty and Photobiology*; Horspool, W. M., Song, P.-S., Eds.; CRC Press: Boca Raton, 1995; p 16.
(2) Collin, G. J. *Adv. Photochem.* **1988**, *14*, 135.
(3) Adam, W.; Oppenländer, T. *Angew. Chem.* **1986**, *98*, 659.
(4) Steinmetz, M. G. Photochemistry with Short UV Light. In *Organic Photochemistry*; Padwa, A., Ed.; Marcel Dekker: New York, 1987; Vol. 8; p 67.
(5) Srinivasan, R.; Brown, K. H. *J. Am. Chem. Soc.* **1978**, *100*, 4602.
(6) Inoue, Y. I.; Mukai, T.; Hakushi, T. *Chem. Lett.* **1982**, 1045.
(7) Wen, A. T.; Hitchcock, A. P.; Werstiuk, N. H.; Nguyen, N.; Leigh, W. J. *Can. J. Chem.* **1990**, *68*, 1967.
(8) Wilsey, S.; Houk, K. N., to be submitted, **2001**.
(9) Wilsey, S.; Houk, K. N.; Zewail, A. H. *J. Am. Chem. Soc.* **1999**, *121*, 5772.
(10) Horn, B. A.; Herek, J. L.; Zewail, A. H. *J. Am. Chem. Soc.* **1996**, *118*, 8755.
(11) Diau, E. W.-G.; De Feyter, S.; Zewail, A. H. *Chem. Phys. Lett.* **1999**, *304*, 134.
(12) Fuss, W.; Schmid, W. E.; Trushin, S. A. *J. Am. Chem. Soc.* **2001**, *123*, 7101.
(13) Roquitte, B. C. *J. Phys. Chem.* **1965**, *69*, 2475.
(14) Barker, J. R.; King, K. D. *J. Chem. Phys.* **1995**, *103*, 4953.
(15) Robin, M. B.; Kuebler, N. A. *J. Chem. Phys.* **1966**, *44*, 2664.
(16) Merer, A. J.; Mulliken, R. S. *Chem. Rev.* **1969**, *69*, 639.
(17) Robin, M. B. *Higher Excited States of Polyatomic Molecules*; Academic Press: New York, 1975; Vol. II.
(18) Fuss, W.; Schmid, W. E.; Trushin, S. A. *J. Chem. Phys.* **2000**, *112*, 8347.
(19) Fuss, W.; Hering, P.; Kompa, K. L.; Lochbrunner, S.; Schikarski, T.; Schmid, W. E. *Ber. Bunsen-Ges. Phys. Chem.* **1997**, *101*, 500.
(20) Trushin, S. A.; Fuss, W.; Schmid, W. E. *Phys. Chem. Chem. Phys.* **2000**, *2*, 1435.
(21) Trushin, S. A.; Diemer, S.; Fuss, W.; Kompa, K. L.; Schmid, W. E. *Phys. Chem. Chem. Phys.* **1999**, *1*, 1431.
(22) Fuss, W.; Schmid, W. E.; Trushin, S. A. *ISRAPS Bull.* **2000**, *11*, 7.
(23) Garavelli, M.; Page, C. S.; Celani, P.; Olivucci, M.; Schmid, W. E.; Trushin, S. A.; Fuss, W. *J. Phys. Chem. A* **2001**, *105*, 4458.
(24) Holmes, J. L.; McGillivray, D. *Org. Mass Spectr.* **1971**, *5*, 1349.
(25) Klessinger, M.; Michl, J. *Excited States and Photochemistry of Organic Molecules*; VCH: New York, 1995.
(26) Evleth, E. M.; Sevin, A. *J. Am. Chem. Soc.* **1981**, *103*, 7414.
(27) Ohmine, I. *J. Chem. Phys.* **1985**, *83*, 2348.
(28) Fuss, W.; Lochbrunner, S.; Müller, A. M.; Schikarski, T.; Schmid, W. E.; Trushin, S. A. *Chem. Phys.* **1998**, *232*, 161.
(29) Freund, L.; Klessinger, M. *Int. J. Quant. Chem.* **1998**, *70*, 1023.
(30) Ben-Nun, M.; Martínez, T. J. *Chem. Phys.* **2000**, *259*, 237.
(31) Mestdagh, J. M.; Visticot, J. P.; Elhanine, M.; Soep, B. *J. Chem. Phys.* **2000**, *113*, 237.
(32) Kirmse, W.; Meinert, T.; Modarelli, D. A.; Platz, M. S. *J. Am. Chem. Soc.* **1993**, *115*, 8918.
(33) Freeman, P. K.; George, D. E.; Rao, V. N. M. *J. Org. Chem.* **1964**, *29*, 1682.
(34) Sulzbach, H. M.; Platz, M. S.; Schaefer, H. F.; Hadad, C. M. *J. Am. Chem. Soc.* **1997**, *119*, 5682.
(35) Siebrand, W.; Dedonder-Lardeux, C.; Jouvet, C. *Chem. Phys. Lett.* **1990**, *174*, 558.
(36) Wickramaaratchi, M. A.; Preses, J. M.; Weston, R. E., Jr. *Chem. Phys. Lett.* **1985**, *120*, 491.
(37) Hirayama, F.; Lipsky, S. *J. Chem. Phys.* **1975**, *62*, 576.
(38) Collin, G. J.; De Maré, G. R. *J. Photochem.* **1987**, *38*, 205.
(39) Benzler, J.; Linkersdörfer, S.; Luther, K. *J. Chem. Phys.* **1997**, *106*, 4992.